Spreading of Thin Films of Ordered Nonionic Surfactants. Origin of the Stepped Shape of the Spreading Precursor

Fredrik Tiberg*,† and Anne-Marie Cazabat

Physique de la Matière Condensée, Collège de France, 11 place Marcelin Berthelot, 75 231 Paris Cedex 05, France

Received December 21, 1993. In Final Form: May 3, 1994®

We report on the phenomenon of surface-induced self-assembly, observed as nonionic siloxane poly(ethylene oxide) surfactants spread at the solid–air interface. Microdroplets of pure surfactants are put on high- and low-energy solid surfaces and the shape evolution is monitored by ellipsometry. Spreading, if any, occurs through an autophobic thin precursor film growing at the foot of the nonwetting main drop. Strikingly different shapes of the precursors are observed, depending on the interfacial properties of the substrate. No specific structure appears as the surfactants spread over high-energy surfaces. On low-energy surfaces, however, these molecules assemble into a densely packed bilayer with long-range intrinsic order. Stratified or "stepped" precursors are seen on medium-energy surfaces. The profile of the precursor is the outcome of the relative strengths of the substrate–surfactant and surfactant–surfactant interaction potentials as well as the molecular dynamic picture within the layer precursor. The area covered by the spreading film always increases linearly with time, yielding apparent diffusion coefficients that are sensitive to surfactant composition, surface chemistry, and perhaps most importantly to the atmospheric humidity. The ability of the surfactants to form dense bilayers is related to the geometry of the molecule, while the sensitivity to humidity is caused by specific interactions between the ethylene oxide part of the surfactants and water. Spreading on low-energy surfaces is observed for surfactants with trisiloxane hydrophobes and relatively short ethylene oxide chains, but not for corresponding hydrocarbon surfactants. This is argued to be the consequence of the relative bulkiness of the trisiloxane hydrophobe allowing space for the hydrophilic ethylene oxide chain and the high density of external hydrophobic methyl groups on the siloxane backbone. The conjunction of these properties may explain the "superspreading" ability of these trisiloxane surfactants.

Introduction

Spreading underlies many important processes and the key problem is often to maximize the speed and uniformity of wetting. Surfactants and copolymers are frequently employed to aid and control the rate of this process. The fashion by which amphiphilic molecules spread over solid surfaces is, however, at present not well understood. This is to a large extent a consequence of the fact that bulk properties usually do not govern the spreading of these molecules. Instead, it is often controlled by local parameters, due to the tendency of these molecules to assemble into different types of organized structures at the interface.

Trisiloxane poly(ethylene oxide) surfactants are for wetting purposes some of the most efficient agents found to date. Several studies show that these surfactants strongly enhance pesticide penetration into foliage of a wide variety of plant species.[1-3] They are also commonly used in lubricants, textile manufacture, cosmetic formulations, and polyurethane foams. Indeed, for wetting applications they are often more potent than for instance fluorocarbon surfactants, which have substantially lower surface tension.[4,5] Their extraordinary ability of promoting water to rapidly spread on hydrophobic surfaces (often referred to as "superspreading") deserves and has lately received scientific interest. The spreading mechanism is, however, still largely unexplained.

Ananthapadmanabhan et al.[5] performed wetting and spreading studies of several different surfactant–water mixtures and proposed a mechanism that relates the spreading capacity of the siloxane surfactant to the particular hammer-shaped geometry of these molecules. This mechanism was later at least partly rejected by Zhu et al.,[4] who showed that "superspreading" was not unique for the hammer-shaped molecules. Instead, they found that dispersion-forming surfactants are better spreading agents than those that formed clear micellar solutions, but this observation does not explain the special status of siloxane surfactants as wetting agents.

The aim of the present study is to perceive the mode of the spreading of neat surfactants on high- and low-energy surfaces. A series of ethoxylated siloxane surfactants with different compositions is studied in order to extract information about molecular properties critical for spreading. Additional studies of similar nonionic surfactant systems are also performed. We show that the structure and intrinsic order of the spreading layer vary strongly with the characteristics of the surface, and that atmospheric water significantly enhances the rate of spreading. These observations are crucial for understanding the spreading mechanism of amphiphilic molecules on solid surfaces and may also shed light on "superspreading" phenomenon discussed in ref 4 and 5.

Experimental Section

Precursor profiles and spreading dynamics were obtained from microdroplet spreading data measured by spatially resolved ellipsometry. This very powerful technique gives precise information about the local thickness as long as the local slope of the drop interface is not too

† Permanent address: Physical Chemistry 1, Chemical Center, University of Lund P.O. Box 124, S-221 00 Lund, Sweden.

® Abstract published in *Advance ACS Abstracts,* June 15, 1994.

(1) Zabkiewicz, J. A.; Gaskin, R. E. In *Adjuvants and Agrochemicals*; Chow, N. P.; Grant, C. A.; Hinshalwood, A.; Sigmundsson, E.; Eds.; CRC Press: Boca Raton, FL, 1989; Vol. 1, pp 141.

(2) Gaskin, R. E.; Kirkwood, R. C. In *Adjuvants and Agrochemicals. Mode of Action and Physiological Activity*; Chow, N. P.; Grant, C. A.; Hinshalwood, A.; Sigmundsson, E.; Eds.; CRC Press: Boca Raton, FL, 1989; Vol. 1, pp 129.

(3) Knoche, M.; Tamura, H.; Bukovac, J. *J. Agric. Food Chem.* **1991**, *39*, 202.

(4) Zhu, X.; Davis, H. T.; Miller, W. G.; Scriven, L. E. *Colloids Surfaces*, submitted for publication.

(5) Ananthapadmanabhan, K. P.; Goddard, E. D.; Chandar, P. *Colloids Surfaces* **1990**, *44*, 281.

0743-7463/94/2410-2301$04.50/0

Table 1. Molecular Formula, Source, and Shape of Surfactants Used in This Study

surfactant	molecular formula	source
$M(D'E_8)M^a$	$((CH_3)_3SiO)_2Si(CH_3)(CH_2)_3(OCH_2CH_2)_8OH$	Dow Corning Corp.
$M(D'E_{12})M^a$	$((CH_3)_3SiO)_2Si(CH_3)(CH_2)_3(OCH_2CH_2)_{12.5}OH$	Dow Corning Corp.
$M(D'E_{16})M^a$	$((CH_3)_3SiO)_2Si(CH_3)(CH_2)_3(OCH_2CH_2)_{16}OH$	Dow Corning Corp.
$MDM'E_8{}^b$	$(CH_3)_3Si(OSi(CH_3)_2)_2(CH_2)_3(OCH_2CH_2)_{7.8}OH$	Dow Corning Corp.
$M(D'E_{10}OD'E_{10})M$	$(CH_3)_3Si(OSi(CH_3)(CH_2)_3(OCH_2CH_2)_{10}OH)_2OSi(CH_3)_3{}^c$	Petrarch Systems
$C_nE_m{}^b$	$CH_3(CH_2)_{n-1}-(OCH_2CH_2)_mOH$ ($n = 12$, $m = 4$, 5, and 8)	Nikko

[a] Hammer-shaped surfactants. [b] Linear-shaped surfactants. [c] Approximate structure of "graft copolymer" PSO71 from Petrarch Systems (MW ≈ 1200, ethylene oxide content = 75 wt %, according to the manufacturer).

Table 2. Values of the Critical Surface Tension (γ_c)[7] Measured at 25 °C with a Series of Alkanes

surface	γ_c/mN m^{-1}
DDTCSB	≈20.6
HMDSB	21.5–23
HMDSA	23–26

steep. The instrument used is a single-wavelength, polarization-modulated ellipsometer that has a focused measurement spot (lateral resolution ≈ 30 μm) and works at the Brewster angle. The optical thickness resolution is 0.2 Å with a time constant of 100 ms for detection. The experimental setup is described elsewhere.[6]

The linear and hammer-shaped surfactants used in this study are presented in Table 1. The hydrophobizing agents, hexamethyldisilazane (HMDS) and dodecatrichlorosilane (DDTCS), were all purchased from Petrarch Systems. Two methods of surface modifications were used: (1) The silicon wafers were first cleaned over 1 h by UV light in oxygen atmosphere. They were then exposed HMDS for 30 min to 3 h in a closed reactor at room temperature and pressure resulting in critical surface tension values (γ_c) in the range shown in Table 2. The precise value depends on the exposure time as well as other factors such as the temperature and pressure in the reactor. These wafers are referred to as HMDSA type surfaces. (2) The second treatment involves the same UV–ozone cleaning procedure, although this was extended to include 15 extra minutes of UV light exposure in oxygen atmosphere saturated with water. The wafer was then put in the reactor, which was evacuated of air by means of a water suction pump. Evacuation was constantly performed during the first 5 min of the HMDS exposure. This procedure results in wafers referred to as HMDSB-type wafers with lower critical surface tension values. Wafers called DDTCSB-type wafers originate from the same grafting procedure but DDTCS has replaced HMDS and the grafting is carried out at a slightly elevated temperature (≈60 °C). These wafers have very low γ_c.

The surfaces were characterized using different techniques. Critical surface tension (γ_c) values were obtained from data on contact angles of a series of alkanes according to the method described by Zisman et al.[7] Typical values on γ_c obtained by this method are presented in Table 2. We also performed a series of water adsorption isotherms on HMDSB, HMDSA, and bare silica. The results are presented in Figure 1. The ellipsometric setup for measuring these is described in ref 8. The difference in hydrophobicity of the HMDSB, HMDSA, and bare wafers is clearly seen in this graph. The amount of water adsorbed on the HMDSB surfaces is very low; less than 0.5 Å is adsorbed at pressures below 13 mmHg (corresponding to a relative humidity ≈93%). The adsorption

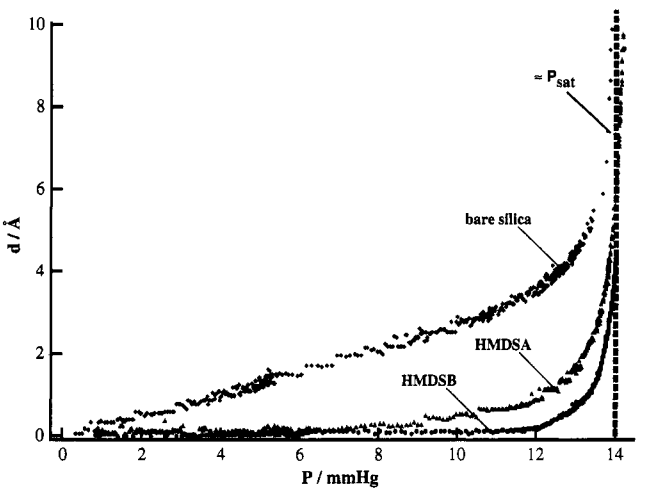

Figure 1. Adsorption isotherm of water on bare silica, HMDSA, and HMDSB. The saturation pressure (P_{sat}) is approximately 14 mmHg. Note that we oversaturated the measurement cell. Therefore, in the case of the HMDSA and HMDSB surfaces, the large thickness of the water layers observed near above P_{sat} corresponds to the condensation of water droplets and not that of a continuous water film.

is slightly higher on HMDSA and more so on bare silica. The bulk part of the results presented in this report will concern spreading on high- (bare silica) and low-(HMDSB) energy surfaces, which in terms of long-range order in the precursor represents the two extremes, see below.

The spreading of the surfactant films was further monitored at different humidities. This was possible by keeping the substrates in chambers with controlled humidity. The regulation of this parameter was done by allowing the air in the box to equilibrate with aqueous solutions of different concentrations of sulfuric acid. The relative humidity (RH) could by this procedure be controlled with an accuracy better than ±5%.

Results

Spreading of nonionic surfactants on solid surfaces, if any, occurs by way of a thin autophobic precursor growing at the foot of the nonwetting main drop. The shape and the degree of intrinsic order of this precursor is strongly affected by the chemistry of the surface. Figure 2 shows the shape of the spreading precursor of $M(D'E_8)M$ at surfaces with progressively increasing surface energies (RH ≈ 30 ± 5%). The top graph shows the spreading from a drop of $M(D'E_8)M$ placed on a low-energy HMDSB wafer. The precursor has on this surface a constant thickness ≈55 Å. This may be compared to the extended length of the molecule, which approximately 35 Å. Figure 2, parts b and c, shows the spreading of same surfactant, but on the less hydrophobic HMDSA surface. Here, the wafers were exposed to HMDS for 90 and 30 min, respectively. The reaction was performed according to the procedure discussed in the Experimental Section. These wafers have higher surface energies than the HMDSB surface, and

(6) Heslot, F.; Cazabat, A. M.; Levinson, P.; Fraysse, N. *Phys. Rev. Lett.* **1990**, *65*, 599.
(7) Zisman, W. A. In *Advances in Chemistry Series*; Gould, R. F.; Ed.; American Chemical Society: Washington, DC, 1964; Vol. 43, pp 1–51.
(8) Levinson, P.; Valignat, M. P.; Fraysse, N.; Cazabat, A. M.; Heslot, F. *Thin Solid Films* **1993**, in press.

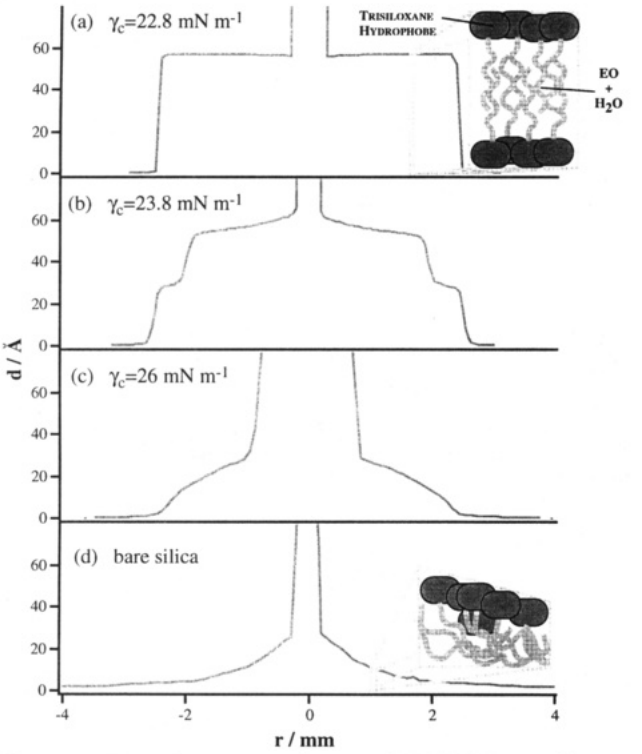

Figure 2. Typical precursor shapes of M(D'E$_8$)M spreading on (a) HMDSB, (b) HMDSA (90 min HMDS exposure), (c) HMDSA (30 min HMDS exposure), and (d) bare silica.

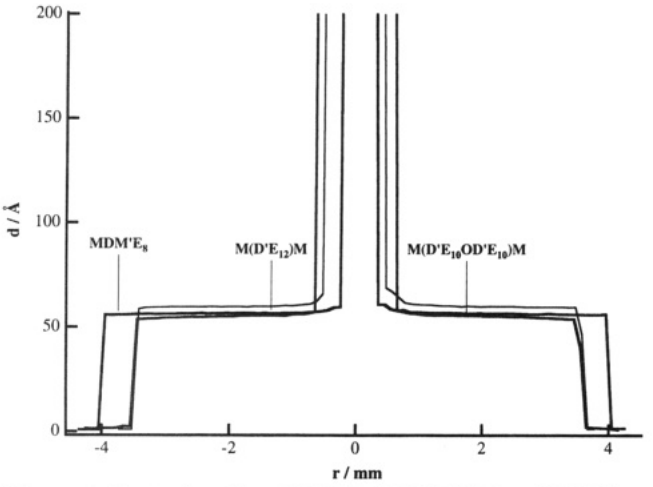

Figure 3. Typical profiles of M(D'E$_{12}$)M, MDM'E$_8$, and M(D'E$_{10}$-OD'E$_{10}$)M drops deposited on a HMDSB surfaces after ≈24 h spreading (RH ≈ 90%).

this has large impact on the shape of the spreading film. Two clear steps ($d \approx 27$ Å) are seen in the upper graph, while only one step with the same final thickness is seen in the lower. Figure 2d finally shows the shape of the film spreading on bare silica. The stepped shape has now disappeared and the precursor looks more as a "sand pile" with a clear shoulder also located around 27 Å. It is clear from these figures that the architecture of the spreading film depends strongly on the chemical composition of the surface.

Typical precursors after a few days spreading of the "hammer"-shaped M(D'E$_{12}$)M and M(D'E$_{10}$OD'E$_{10}$)M surfactants, which have larger poly(ethylene oxide) portions, as well as the linear MDM'E$_8$ trisiloxane on HMDSB surfaces are also shown in Figure 3. The profiles of the spreading film of these surfactants are clearly more or less identical with that observed for M(D'E$_8$)M. The

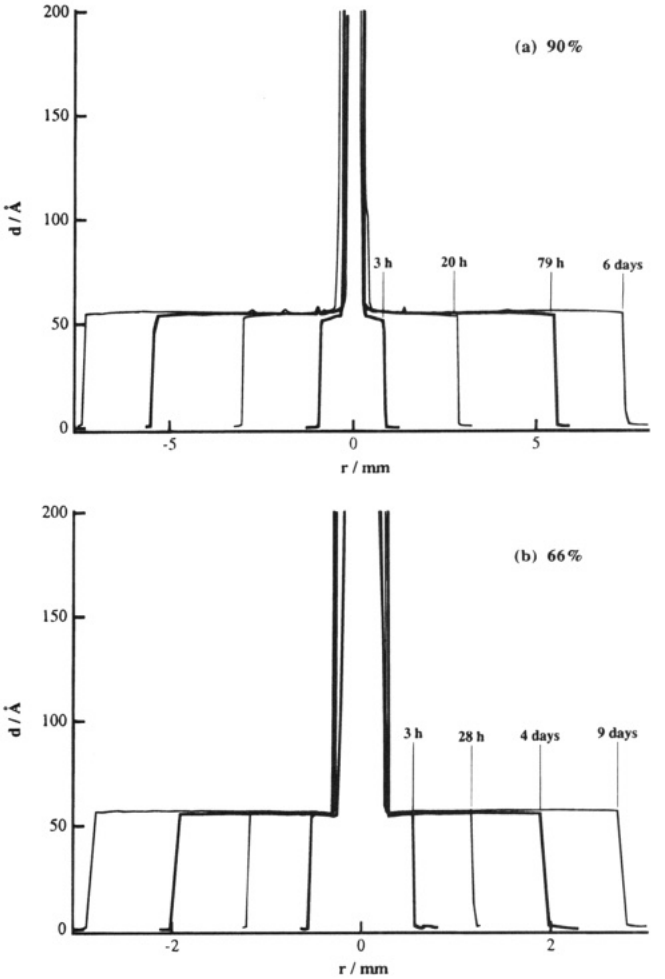

Figure 4. Evolution of the drop profile of M(D'E$_8$)M spreading over HMDSB at (a) 90% and (b) 66% relative humidity.

thickness, however, is 4−6 Å larger for M(D'E$_{12}$)M than for the others.

The evolution of the precursor on HMDSB surfaces at high and low relative humidities are exemplified in Figure 4, parts a and b. Here the shape of a M(D'E$_8$)M precursor is shown at progressively increasing times after the drop deposition. The change in the relative humidity of the surrounding atmosphere from 90% to 66% causes an substantial decrease in the rate of spreading, but has no visual effect on the spreading precursor characteristics. The radius of the precursor grows steadily with time, while the thickness and the general shape remain virtually constant.

Figure 5 shows the evolution of a M(D'E$_8$)M drop deposition on an HMDSA surface ($\gamma_c = 23.8$ mN m^{-1}) with time. The time dependence resembles that observed on the HMDSB surface. Both layers expand steadily with time and very small changes are observed in the thickness of each layer as well as the shape of the precursor profile.

While low-energy (HMDSB) surfaces induce close to perfect long-range intrinsic order of the spreading precursor, spreading on bare silica represents the other extreme. An autophobic precursor extending out from the foot of the main drop is observed also in this case, but the spreading occurs in a more disorganized fashion resulting in the "sand pile"-shaped precursors shown for M(D'E$_8$)M in Figure 6. A leading thin film (a few ångströms high) of scattered individual or aggregated M(D'E$_8$)M molecules quickly covers the entire surface. As the main drop is approached, the thickness of this film increases smoothly to a final height of about 27 Å, observed at the transition

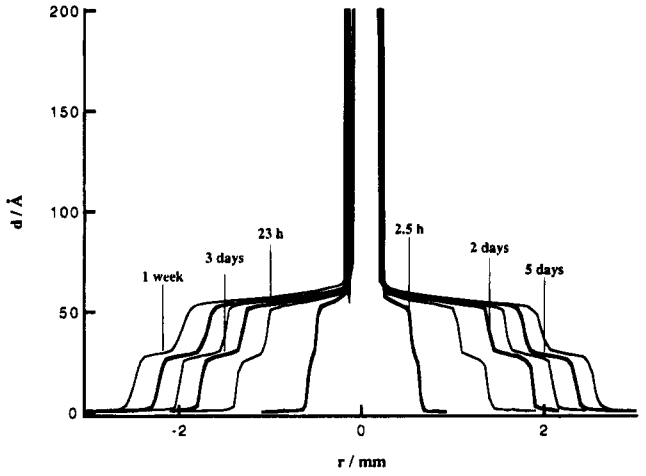

Figure 5. Evolution of the drop profile of M(D'E$_8$)M spreading over HMDSA at 30% relative humidity.

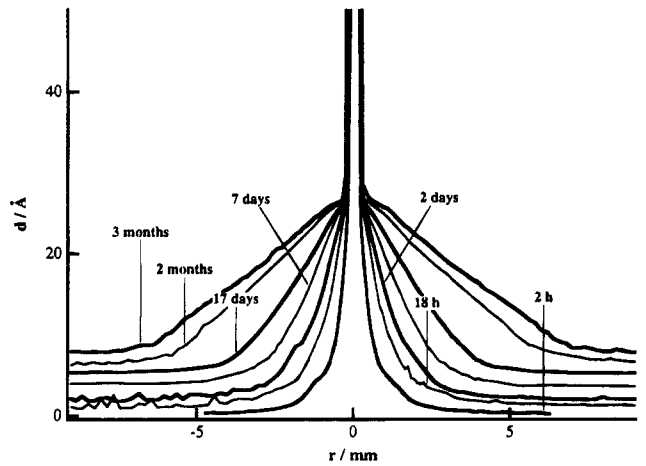

Figure 6. Evolution of the drop profile of M(D'E$_8$)M spreading over bare silica at 30% relative humidity.

to the main drop. M(D'E$_{12}$)M spreads in a similar fashion on bare silica. The thickness of the M(D'E$_{12}$)M precursor at the transition to the main drop is the same, and the shape differs merely in details (results not shown).

The radius (r) of the precursor, measured at a fixed distance from the surface and at constant relative humidity, always increases linearly with the square root of the time, thus following a $r = r_0 + D_{app}t^{1/2}$ law. This relation holds until the central reservoir is nearly emptied, when the spreading decelerates and finally reaches a standstill. Figure 7 shows the radius of M(D'E$_8$)M precursors (measured 10 Å above the surface or the plateau of the first layer) spreading on HMDSB and HMDSA surfaces plotted against the square root of time (RH = 30%). D_{app} can easily be estimated from the slope of such curves.

The influence of the relative humidity (RH) on the spreading of surfactants over HMDSB surfaces is rather large as can be seen in Figure 7a. Moreover, Figure 8 shows that the relation between D_{app} and RH is rather general for all the surfactants that were found to spread on this surface. A slight increase in D_{app} is observed in the interval up to RH values of 65–70%, and then the spreading rates are drastically raised. M(D'E$_{12}$)M does in relative terms spread much slower over the surface than both the "hammer"-shaped M(D'E$_8$)M and the linear MDM'E$_8$ at low humidities. The curves do, however, seem to converge as the humidity is increased above 70%. This effect is more pronounced for M(D'E$_{10}$OD'E$_{10}$)M, which displays a transition from nonspreading to spreading somewhere between 30% and 50% relative humidity. In

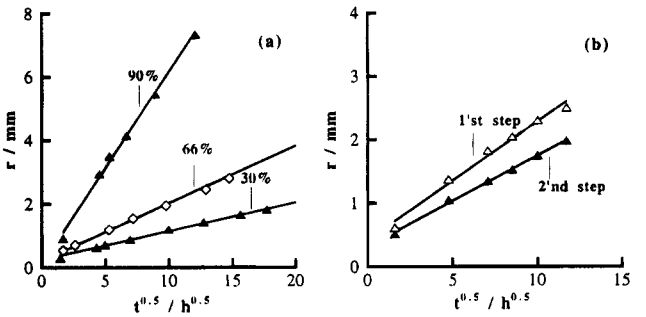

Figure 7. (a) Radius of the drop precursor (r) measured at different humidities as a function of square root of time (t) for M(D'E$_8$)M spreading on HMDSB wafers an (b) time evolution of the radius of the first and the second step seen in Figure 5 (RH = 30%) on a HMDSA surface. The slope of these curves corresponds to the rate of the monolayer and the layer spreading between the monolayer and the surface, see illustration in Figure 9.

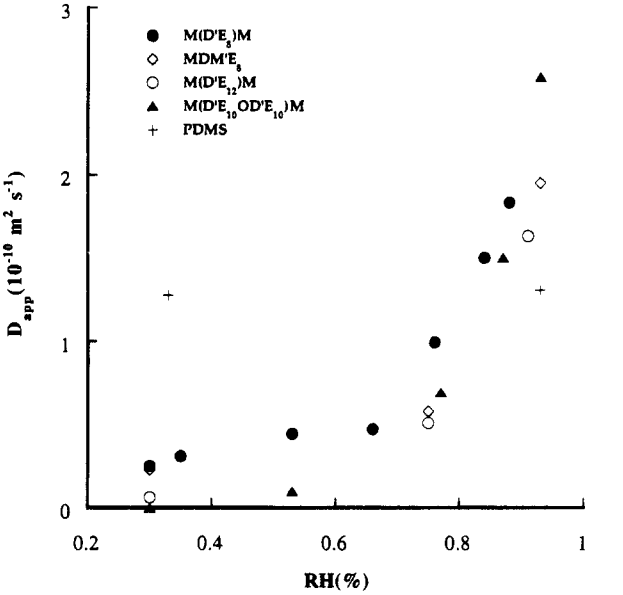

Figure 8. Apparent diffusion coefficient (D_{app}) versus relative humidity (RH) for M(D'E$_8$)M, M(D'E$_{12}$)M, (MDM'E$_8$), M(D'E$_{10}$-OD'E$_{10}$)M, and PDMS spreading on HMDSB wafers.

contrast, M(D'E$_{16}$)M does not spread at any humidities, nor did any of the ethoxylated hydrocarbon surfactants. Note that the M(D'E$_{16}$)M measurements were performed at 35 °C, where M(D'E$_{16}$)M is a low viscosity liquid. We can also see in Figure 8 that the rate of spreading of a 20 cst polydimethylsilane (PDMS) is independent of the atmospheric humidity. The PDMS molecule is chemically similar to the hydrophobic siloxane part of the surfactant molecule, i.e., the one that is in contact with the surface in this case. Spreading on the DDTCSB surface was not observed for any of the surfactants, nor was it observed for the 20 cst PDMS.

The spreading rates of the siloxane surfactants in saturated water vapor atmosphere are too fast to be monitored properly with our method. The profile of the precursor after spreading could, however, be studied, and it was found identical with that observed at lower humidities. Note, that the "superspreading" phenomenon discussed in reference 4 is only observed at high humidities.

Atmospheric humidity affects spreading on bare silica in a way similar to that observed on HMDSB surfaces. The rate of the leading edge of the M(D'E$_8$)M film calculated at any fixed distance (<20 Å) from the surface increases with a factor of about 10, when the relative

humidity of the atmosphere is increased from 30% to 93%. The evolution of the precursor shape is, thus, independent of the surrounding humidity.

Discussion

The spreading process of amphiphilic molecules can roughly be divided into two steps: (i) transport to and organization at the interface of bulk molecules and (ii) the diffusion-like spreading of the precursor over the surface. To fully understand the spreading process we need to perceive the mechanism of film formation and spreading, the forces acting on the spreading precursor, and the role of other molecules (read adsorbed and atmospheric water) in the spreading process.

The structure of the spreading film depends critically on the chemistry of the surface. For spreading to occur on the low-energy HMDSB surface, the surfactants must form a layer with a high interfacial density of hydrophobic siloxane moiety and thereby acquire low local interfacial tensions with respect to both the surface and the surrounding air. The spreading layer has a uniform thickness that is larger than the length of an extended surfactant molecule. Ellipsometric data for $M(D'E_8)M$, give an area per surfactant molecule of around 20 Å^2, which is less than half the area occupied by one $M(D'E_{7.5}OMe)M$ molecule, ≈50 Å^2, adsorbed at the water−polyethylene interface, where monolayer coverage is expected.[5] The latter value also agrees with what is calculated from the projected area of the hydrophobic siloxane head group. This indicates that the spreading layer has bilayer conformation, with the more hydrophilic part of the molecules, the ethylene oxide (E) head groups, located in the interior surrounded by trisiloxane groups, see illustration in Figure 2a. A small increase, ≈5 Å, in the thickness is noticed as the ethylene oxide chain is increased from 8 to 12 on going from $M(D'E_8)M$ to $M(D'E_{12})M$. This indicates that the latter forms a less dense bilayer on HMDSB surfaces, which also might explain the comparatively low spreading rates observed for $M(D'E_{12})M$ at low humidities, see Figure 8. No spreading at all was observed for $M(D'E_{16})M$, which has an even larger hydrophilic to hydrophobic ratio. The effect may be related to the increasing difficulty in forming dense zero-curvature bilayer structures when the length of the ethylene oxide chain increases. This is in good accord with the bulk phase behavior of these and similar surfactants as well as with expectations of preferred aggregates according to the packing constraint concept.[9-11]

The spreading pattern on bare silica shown in Figures 2 and 6, is very different from that on HMDSB surfaces. The thin leading part of the spreading layers is on this surface most likely built up by surfactants with the ethylene oxide chains strongly tilted toward the surface. The leading part of the layer is initially also rather irregular on bare silica indicating that islands of such molecules cover the surface. With time, however, the surface coverage increases. The surfactant becomes progressively less tilted as the foot of the main drop is approached, see Figure 2d. Thus, while low-energy surfaces promote long-range intrinsic order of the spreading precursor, spreading on high-energy surfaces occurs in a more disorganized fashion. The latter can be attributed to the relatively strong adhesion between the ethoxy groups and the silica surface, which outplays surfactant−surfactant interactions promoting order in the precursor.

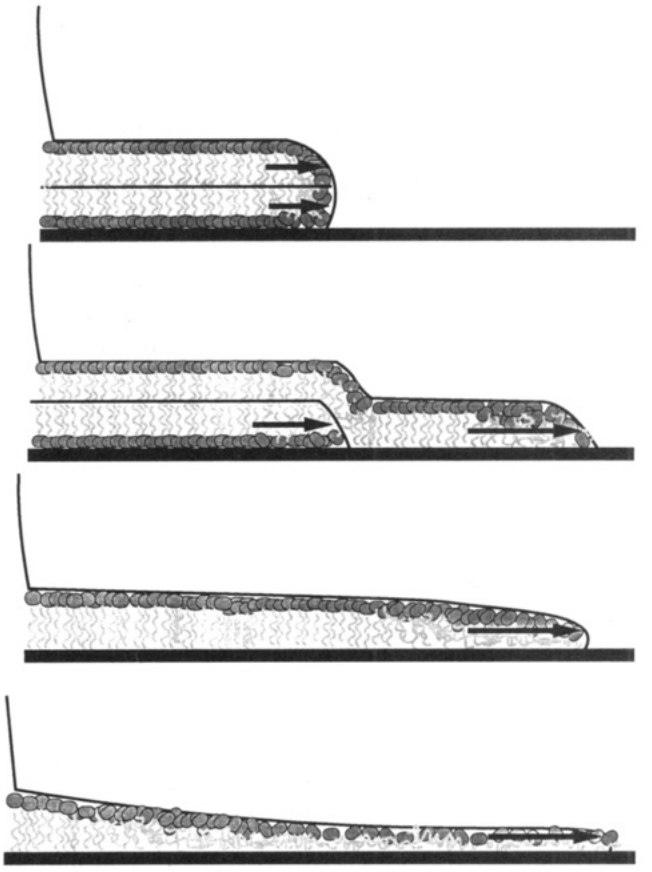

Figure 9. Schematic illustrations of the flow and the conformation of the surfactants within the precursor during spreading. The different pictures correspond to the profiles given in Figure 2.

The interpretation of the spreading behavior obtained on HMDSA type wafers is a more delicate problem and the discussion will be of a somewhat speculative nature. A transition from a precursor with one extended step to a spreading film with two rather distinct steps is observed as the critical surface tension decreases from 26 to 23.8 mN m^{-1}. The profile of the precursor is the outcome of molecular dynamic events and the relative strength of short-range intermolecular forces acting within the spreading film as well as between the film and the surrounding media.

We picture the spreading processes as shown in Figure 9. These drawings correspond to the different profiles shown in Figure 2. Here, we assume that the flux in the precursor is dominated by one-dimensional flow parallel to the surface. The different layers in the precursor, thus, move with a characteristic rate and any exchange of matter between the two layers is slow. We also presume that the main conformational features of the advancing layer on bare silica and the HMDSB surface are correctly pictured in the inserts in Figure 2 part a and d.

When adhesion between the surface and the ethoxy groups of the surfactants decreases and intersurfactant interaction becomes more important, ordering within the monolayer is expected to increase. This is exactly what we observe as the surface energy decreases, see Figure 2. However, at one point, as the adhesion between the ethoxy groups and the surface starts to diminish, another layer starts to spread in between the single monolayer and the surface. The hydrophobic siloxane groups are in this layer

(9) He, M.; Hill, R. M.; Lin, Z.; Scriven, L. E.; Davis. H. T. *J. Phys. Chem.* **1993**, *97*, 8820.
(10) Mitchell, J. D.; Tiddy, G. J. T.; Waring, L.; Bostock, T.; McDonald, M. P. *J. Chem. Soc., Faraday Trans. 1* **1983**, *79*, 975.
(11) Israelachvili, J. *Intermolecular & Surface Forces*.; 2 ed.; Academic Press Limited: New York, 1991.

oriented against the hydrophobic surface as indicated in Figure 9. A precursor having two steps is then a consequence of different spreading rates of these individual layers, see Figures 5 and 7b. Finally, the monolayer step disappears as the energy of the surface becomes too low for this layer to advance by itself over the surface. This results in the characteristic bilayer profile with sharp edges seen in Figures 2–4.

The spreading rate of the advancing single monolayer was observed to be almost the same on silica and the HMDSA surface (for three different two-step profiles and one one-step profile). The diffusion coefficient D_{app} was in all cases around 5.5×10^{-11} m^2 s^{-1} (RH=30%). The rate of the second layer, on the other hand, increases with decreasing surface energy to rates close to that of the monolayer, consistent with decreasing adhesive forces between the single monolayer and the surface. The rate of both layers then drops to a rather steady value ($D_{app} \approx 2.7 \times 10^{-11}$ m^2 s^{-1}, RH = 30%) as the monolayer no longer can spread by itself on the surface.

Surface properties are shown to strongly modify the precursor profile and, hence, also the flow pattern within the spreading film. The composition of the surfactant and the humidity of the surrounding air also affects the spreading, as can be seen in Figure 8. However, changing these parameters only affects the rate of spreading and not the resulting shape of the spreading precursor, see Figure 4, parts a and b. To explain the increase in D_{app} with humidity this behavior it is necessary to consider the driving forces for spreading. Generally, D_{app} is the ratio between a driving term promoting spreading and a friction term.[12,13] This can for a film of constant thickness be written as W_1/ξ, where W_1 and ξ are the local potential of the film with reference to the main drop and the molecular friction, respectively. The increase in D_{app} could be explained by a reduction of ξ between the adsorbed layer and the surface, due to the presence of adsorbed water. This does, however, seem unlikely, considering that the shape of the precursor remains the same and because the isotherms show that less than 0.5 Å of water is adsorbed on HMDSB wafers at RH values under 90%. Another observation that opposes this hypothesis is the fact that the spreading rate of PDMS (a polymer with chemical characteristics similar to that of the hydrophobic moiety of the surfactant) is unaffected by humidity, see Figure 6. Hence, it appears as if the increasing spreading rates are not a consequence of decreasing ξ values between the spreading film and the surface, but instead involve interactions between atmospheric water and interior hydrophilic ethylene oxide groups. D_{app} provides an estimate of this effect and since the main driving term for spreading is the difference in chemical potential between the edge of the film and the main drop (a Marangoni term), D_{app} must be proportional to this difference.

Note that Zhu et al.[4] found a similar dependence for the spreading of binary solutions of M(D'E$_{7.5}$Me)M–water dispersions, which spread much faster over parafilm when the surrounding air is saturated with water than in a dry atmosphere. They inferred that behavior might be explained by water deposition from the vapor to the leading edge of the spreading film. The spreading film process would then be driven by adsorption solution chemistry in the air–film solid contact regime. A convincing proof for this mechanism was not given, and our data neither opposes nor confirms this notion. The time scale of the spreading is, however, several orders of magnitude higher for the binary surfactant–water case than that observed by us for pure surfactants on hydrophobic surfaces. This means that a comparison between the two cases is difficult.

Increasing the portion of ethylene oxide groups in the surfactant results in a large decrease of the spreading rate at low relative humidities, while no differences or the reverse situation was observed at high humidities, see Figure 8. We believe that the difference in packing constraints manifests itself at low values of the humidity and that this effect is screened by the ethylene oxide–water interactions that become more pronounced with increasing ethylene oxide portion. Note, however, that there is a limiting relative size of the hydrophilic part above which no spreading occurs.

Conclusions

This work shows that the spreading of amphiphilic molecules is a process full of nuances, where a subtle change of the surface properties greatly modifies the mode of spreading. For surfaces with critical surface tensions in the interval from 26 to around 22 mN m^{-1}, the structure of the spreading precursor changes from monolayer to coexisting mono- and bilayers and finally to a single well-defined bilayer. Crucial for the shape and structure of the precursor is the contention between surfactant–surfactant interactions and adhesive forces between the hydrophilic parts of the surfactant and the surface. Also important is the molecular dynamics picture within the spreading precursor. Another observation was that atmospheric water strongly enhances the rate of spreading, yet it has no effect on the profile of the precursor. This is a consequence of specific water–ethylene oxide interactions, but the exact nature of these is not understood. To execute quantitative expressions for these observations is a challenging task that yet has to be realized.

Spreading on low-energy HMDSB surfaces, finally, requires that certain criteria are fulfilled regarding the chemistry and microstructure of the surfactant. This includes the presence of a siloxane hydrophobic group and a relatively short hydrophilic chain. The latter is necessary to provide the means for the surfactant to form zero-curvature bilayers with a high interfacial density of hydrophobic methyl groups. The criteria for spreading and the dependence on humidity are all consistent with observations by Zhu et al.[4] on the binary surfactant–water system.

Acknowledgment. The authors thank Paul Levinson for performing adsorption isotherms and Bengt Jönsson (University of Lund) and Ted Davis (University of Minnesota) for very enlightening discussions on this topic. Randy Hill (Dow Corning Corp.), Desmond Goddard (Union Carbide Corp.), and Martin Hellsten (Berol Nobel) are also acknowledged for providing us with the surfactants used in this work. F.T. was sponsored by the Swedish Institute (SI) and the Swedish National Board for Technical Development (NUTEK).

(12) Fraysse, N.; Valignat, M. P.; Cazabat, A. M.; Heslot, F.; Levinson, P. *J. Colloid Interface Sci.* **1993**, *158*, 27.

(13) de Gennes, P. G.; Cazabat, A. M. *C. R. Acad. Sci. Paris* **1990**, *310*, 1601.